FUDMA Journal of Sciences (FJS)
ISSN online: 2616-1370
ISSN print: 2645 - 2944
Vol. 9 No. 2, February, 2025, pp 220 - 230
DOI: https://doi.org/10.33003/fjs-2025-0902-3176

ISOLATION, CHARACTERIZATION AND EVALUATION OF ANTIOXIDANT ACTIVITY OF SILICA CELLULOSE NANOCOMPOSITE (SiO_2-CNC) EXTRACTED FROM BIO-WASTE (RICE HUSK) INTEGRATED WITH CALLISTEMON CITRINUS EXTRACT

[1]Adegbe Amanabo Monday, *[1]Larayetan Rotimi Abisoye, [2]Omatola Kingsley Makoji, [1]Onoja Ceaser William, [1]Abah Sunday, [1]Abu Arome, [3]Abalaka Daniel Hassan and [4]Ogunmola Oluranti Olagoke

[1]Department of Pure and Industrial Chemistry, Kogi State University, Kogi State, Anyigba, Nigeria
[2]Department of Physics, Kogi State University, Kogi State, Anyigba, Nigeria
[3]School of Applied Sciences, Department of Science Laboratory Technology, Kogi State Polytechnic Lokoja, Kogi, Nigeria
[4]Chemistry unit, department Of Physical Sciences Education, Emmanuel Alayande University of Education, P.M.B 1010, Oyo, Nigeria

*Corresponding authors' email: timlarayetan@gmail.com Phone: +2348030510909

ABSTRACT

Recent research has focused on more complex uses, such as the extraction of silica cellulose nanocomposite from rice husks, which has potential as a way to create high-tech materials. The work describes the successful isolation, characterization, and assessment of rice husk-derived silica cellulose nanocomposite (SiO_2-CNC) with *Callistemon citrinus* extract integration. The synthesis process consisted of three principal operations: delignification with alkaline treatment, sodium hypochlorite bleaching, and concentrated sulphuric acid hydrolysis. The prepared nanocomposite was analyzed by EDX, SEM, TEM, FTIR, spectrophotometry, and thermal analysis (DTA/TGA). EDX studies showed a composite material with elemental silica (40.20%), carbon (20.76%), silver (10.57%), and zinc (8.50%) in significant proportions. The sophisticated material structure with uniform porous networks was demonstrated by SEM analysis, while the presence of nanoparticles sized from 2.70 to 6.37 nm was confirmed by TEM. Thermal analysis showed distinct decomposition steps beyond 250ºC, and material stability was observed up to these temperatures. FTIR spectroscopy verified the functional groups in SiO_2-CNC and the rice husk extract, while UV analysis showed strong absorption in the 200-230 nm range. *Callistemon citrinus* extract showed the ability to enhance the antioxidant properties of SiO_2-CNC, which was observable in DPPH and ABTS assays. The integrated composite showed significant DPPH and ABTS radical scavenging activities. These findings demonstrate the successful conversion of agricultural waste into a value-added nanocomposite with enhanced functional properties, offering potential application in antioxidant delivery systems, and advanced materials development. This research contributes to sustainable nanomaterial development while addressing agricultural waste management challenges.

Keywords: Rice-husks, Silica cellulose nanocomposite (SiO_2-CNC), EDX, SEM, TEM, FTIR

INTRODUCTION

Recent studies have explored various methodology for developing eco-friendly composite materials utilizing agricultural waste. These approaches focuses on material selection, treatment processes, fabrication techniques and comprehensive characterization to ensure sustainability and performance. The development of eco-friendly composite materials from agricultural waste biomass for sustainable development has gained significant attention due to environmental challenges and the demand for eco-friendly manufacturing (Phiri *et al*. 2023). In Nigeria, with rice husk accounting for 20% of total production (Salihu Makanta, 2021). On a global scale, rice is one of the most important food crops that is cultivated in more than 100 countries, producing more than 715 million tonnes of paddy rice every year. As of 2019, Nigeria's rice output hit 8.34 million tonnes (Ahmed, 2019). Poor management of rice husk (RH) disposal through burning has serious consequences for the environment, including worsening human respiratory diseases and contributing to methane emissions during RH decomposition (Piyathissa *et al.*, 2023). Rice husk (RH) is the protective shell of rice grains, composed of four layers: structural, fibrous, sponge-like, and cellular. The main constituents of RH are cellulose (35%), hemicellulose (25%), lignin (20%), crude protein (3%), and inorganic compounds (17%) (Nguyen *et al*., 2022). Replacing limited renewable fuel sources with rice husk is an efficient way to enhance traditional uses (Requena *et al.* 2019), as well as using it as a filler in bioplastics (Jannah *et al.,* 2019) and partially substituting it into construction materials (Ghosal & Moulik, 2015). New research has been directed toward more sophisticated uses, such as the extraction of silica cellulose nanocomposite (SiO_2-CNC) from rice husks, which is a promising way to create high-tech materials (Ates *et al.*, 2020; Teo & Wahab, 2020). These nanocrystals, when incorporated with bioactive plant extracts such as *Callistemon citrinus*, offer enhanced functionality and potential applications in various fields. The properties of these bio-based nanocomposites are influenced by several key parameters, including processing conditions and temperature (Khan *et al*., 2021). Studies have shown that the material properties of integrated components are superior in value, which could be due to the strong chemical interactions that occurs between different constituents (Balaji *et al.*, 2024). At the same time, the addition of plant extracts adds more value with their bioactive compounds, especially in terms of antioxidant activity, although it must be properly optimized since too much of any of the components would result in phase separations and lower mechanical properties (Dairi *et al.*, 2019). This change of perception on the rice husk from a waste to a valued material is a classic example of the circular economy and sustainable resource management (Oyejobi *et*

al., 2024). Innovative processing techniques that address the environmental challenges and provide high yields of desirable products are not only solving waste management problems but also creating economic opportunities that are aligned with the sustainability priorities of the world. This study is focused on generating silica cellulose nanocomposite SiO_2-CNC from rice husk, characterizing the SiO_2-CNC using TEM, SEM, FTIR, DTA/TGA, and UV and integrating *Callistemon citrinus* into the SiO_2-CNC and assessing the antioxidant activity of the modified SiO_2-CNC.

MATERIALS AND METHODS

Materials and Reagents

The materials and reagents used for the production of the silica-cellulose nanoparticles are RH obtained from a rice mill plant, sodium hydroxide (NaOH, 96%), sodium hypochlorite (NaOCl), hydrogen peroxide (H_2O_2, 30%), methanoic acid (HCOOH, 90%), and sulphuric acid (H_2SO_4, 98%).

Sample Pre-treatment

Rice husk was obtained from the premises of the Ega rice market in Idah, Kogi State; it was then washed thoroughly with distilled water to remove dirt and impurities, followed by drying the rice husk in an oven at 60°C for 12 hours until a constant weight was achieved. The dried rice husk was then ground with a mechanical grinder (Polymix, PX-MFC 90D) and then stored for further treatment.

Methods

The methodology employed was based on the synthesis of silica-cellulose nanoparticles as highlighted by Hernandez *Perez et al*. (2023), with some slight modifications. Three main processes were engaged in the successive process of isolating silica-cellulose from rice husks (RH).

Delignification Process

Alkaline treatment was used to eliminate lignin and hemicellulose from the rice husk fibres in order to extract pure silica cellulose nanocomposite (SiO_2-CNC). This involved combining 50 grams of powdered rice husks with 400 mL of 12% sodium hydroxide in a 1000 mL beaker. The mixture was then heated at 80°C for 3h and stirred with a magnetic stirrer; next, the mixture was filtered, and the precipitate was washed with distilled water until a neutral pH was obtained.

Bleaching Treatment

The delignification residue was treated with 400 mL of a 2.5% sodium hypochlorite solution, and this mixture was maintained at 80°C and continuously stirred for an hour using a magnetic stirrer. After filtration and washing with distilled water until neutral pH was obtained, the material was allowed to settle for 1 h, yielding the rice husk silica cellulose extract.

Acid hydrolysis (Production of silica-cellulose nanocrystal (SiO_2-CNC)

To make SiO_2-CNC, acid hydrolysis treatment was conducted on the RH cellulose after alkali treatment and bleaching at a temperature of 50 °C using concentrated sulphuric acid for 2 h under continuous stirring (1:20 ratio of solid mass to acid volume). The final product was centrifuged many times at 15,000 rpm for 15 minutes at 10°C. After that, the substance was dialyzed against distilled water until its pH stabilized at a level between 5 and 6, it was then sonicated before being refrigerated.

Characterization

Surface Morphology

The morphological characteristics of the extracted cellulose were examined using a Supra 55-VP FEGSEM Zeiss scanning electron microscope. All samples were gold sputtered for 15 mA for 5 minutes, and SEM imaging was set for the SE2 signal with an electron beam of 4 kV.

Functional Group Analysis

The chemical composition was examined using FTIR spectroscopy with a Nicolet 6700 spectrometer. Samples were prepared on KBr discs, with spectra recorded at 4 cm^{-1} resolution over 32 scans and processed using OMNIC software. (Thermo Fisher Scientific, Inc., USA) software was used to smooth the obtained spectra.

Crystallinity Assessment

The samples were analyzed using an X-ray diffractometer (D8-Advance Bruker AXS GmbH) at room temperature with a monochromatic CuK radiation source (= 0.1539 nm) in the step-scan mode with a 2θ angle ranging from 10° to 50° with a step of 0.04 and a scanning time of 5.0 min. A D2 PHASER system running at 30 kV and 10 mA was utilized for additional examination. It scanned from 10 to 80° at a rate of 0.02° per minute.

Thermal analysis (TGA/DTA)

The temperature stability of the sample was measured with a TGA/DTA thermogravimetric analyser (Mettler Toledo Corporation, Schwarzenbach, Switzerland).

Transmission electron microscopy (TEM)

TEM (JEM-1400 F, JEOL Ltd, Tokyo, Japan) observations were carried out in duplicate at 100 kV accelerating voltage to study the morphology of the treated materials and SiO_2-CNC. Micropipette drops of 1.0 wt% SiO_2-CNC suspension were placed on copper grids, dried at ambient temperature, and examined using TEM.

UV-Vis spectroscopy

The UV–visible spectra of the silica cellulose nanocomposites (SiO_2-CNC) and extract were recorded using a UV-2600 spectrophotometer (SPECORD 250 UV/ VIS, Germany) from 200 to 800 nm.

Extract Integration and Analysis

The silica cellulose nanocomposite (SiO_2-CNC) was combined with Callistemon citrinus extract in equal proportions and stored at 4°C. The mixture is composed of equal parts of each compound, with each compound comprising 50% of the total mixture.

Assessment of the Incorporated SiO_2-CNS's Free Radical Scavenging Activity

The antioxidant activity was measured with DPPH and different concentrations of the mixture were tested (25-125 mgmL-1) as well as reference antioxidants with DPPH in DMSO. After 40 minutes of dark incubation at room temperature, absorption measurements at 517 nm determined the free radical scavenging capacity. Results were calculated using the standard DPPH inhibition formula, comparing sample absorption against controls to determine IC_{50} values.

Where $A_{control}$ is the absorbance of DPPH+DMSO; A_{sample} is the absorbance of DPPH + either incorporated SiO_2-CNS or the synthetic antioxidant agent. Dose-response curve was plotted and IC_{50} value of the synthetic antioxidant

and the incorporated SiO_2-CNS were calculated (Larayetan *et al*., 2021).

By oxidizing ABTS stock solution (7 mM) with 2.4 mM potassium persulfate in equal proportions, the operational solution was obtained. The mixture was then left to react for 12 hours at room temperature. A UV spectrophotometer was used to measure the absorbance at 734 nm (0.706 ± 0.001) upon 7 minutes after adding 60 mL of methanol to a fraction of the resultant solution (1 mL). In short, each extract was added to the methanol solution of ABTS at different concentrations (0.025 to 0.4 mg/mL) and left for seven minutes at room temperature in the dark. After that, absorbance was measured spectrophotometrically at 760 nm, and the equation for DPPH was used to determine the ABTS% inhibition caused by the extracts and commercial antioxidant (vitamin C) (Larayetan *et al*., 2021).

RESULTS AND DISCUSSION

EDX Analysis of Silica-Cellulose Nanocomposite

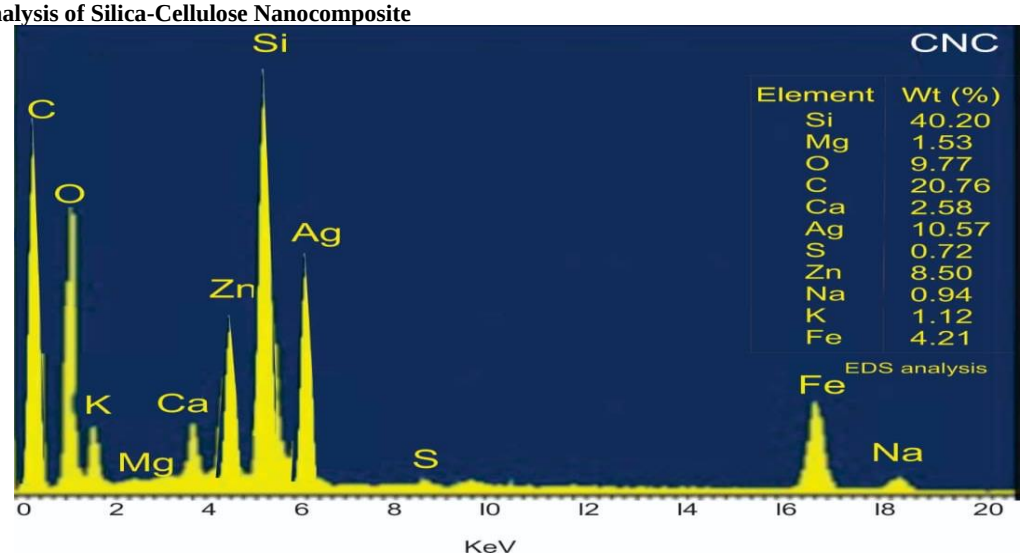

Figure 1: EDX analysis of silica-cellulose nanocomposite (SiO_2-CNC)

This is an analytical technique used for elemental analysis and chemical characterization of materials, usually coupled with SEM or TEM, its principles is based on the interaction between an electron beam and a sample, causing inner shell electrons in atoms to be ejected which results in the emission of characteristic X-rays specific to each element detected by a silicon drift detector, this converts the energy of the X-rays into electrical signals that are processed into elemental spectrum. The energy-dispersive X-ray (EDX) spectroscopy analysis of the silica-cellulose nanocomposite from rice husk shows a complex elemental composition, with the most prominent being silica (SiO_2) in an approximate weight percentage of 40.20% as can be seen by the highest peak in Fig. 1. Such high silica content is common in materials derived from rice husk, as rice plants naturally accumulate silica during growth. The carbon content of 20.76%, shown by the prominent C peak at the lower energy range, confirms the existence of the cellulose component and successful formation of the organic-inorganic composite structure. The presence of oxygen at 9.77%, visible as a distinct peak between C and Si, suggests the formation of Silica dioxide (silica) and other oxide compounds. Interestingly, the sample contains significant amounts of silver (Ag) at 10.57% and zinc (Zn) at 8.50%, represented by well-defined peaks in the middle region of the EDX spectrum. Zinc is an essential micronutrient for rice plants, playing crucial roles in enzyme activities and protein synthesis (Rehman *et al*., 2012). However, the relatively high concentration might indicate either soil enrichment through fertilizers or natural mineral-rich soil conditions. The presence of silver is less common naturally and might suggest either environmental factors such as industrial activities near the cultivation area or potential contamination during the processing stages (Reidy *et al*., 2013). The presence of various metals in the rice husk-derived silica-cellulose nanocomposite can be attributed to several natural and environmental factors. The notable presence of iron (Fe) at 4.21%, evident from its distinct peak in the higher keV region, can be traced to the soil composition where the rice was cultivated, as iron is one of the essential micronutrients required for plant growth and chlorophyll synthesis. The presence of oxygen at 9.77%, which can be seen as a separate peak between C and Si, suggests the formation of silica dioxide (silica) and other oxide compounds. Interestingly, the sample contains Ag and Zn at 10.57% and 8.50%, respectively, which are marked quite clearly in the midsection of the EDX spectrum. Concentration of the elemental zinc is often regarded as an essential micronutrient for rice plants, with importance in enzyme activities and protein synthesis as well (Rehman *et al*., 2012). In paddy rice fields, iron uptake is necessary in anaerobic conditions where iron is more accessible (Kuan *et al.,* 2012). The analysis confirms even lower amounts of other minerals, which includes calcium (Ca) at 2.58%, magnesium (Mg) at 1.53%, potassium (K) at 1.12%, sodium (Na) at 0.94%, and sulphur (S) at 0.72%. All these components are detectable as smaller peaks on the spectrum. Rice biomass contains these trace elements, and it is probable that they come from natural mineral uptake of rice plants during their growth (Bakare, 2021). The sulphur content (0.72%), visible as a small peak, likely originates from the plant's protein structures and secondary metabolites, as sulphur is essential for amino acid synthesis (Patel *et al.,* 2023).

The successful synthesis of a silica-cellulose nanocomposite while still containing some of the natural mineral parts from the rice husk precursor is confirmed by the presence of these different elements, especially the high silica concentration along with carbon, as clearly demonstrated by the intensity of their peaks (Shen *et al.,* 2014).

SEM Analysis of Silica-Cellulose Nanocomposite (SiO_2-CNC)

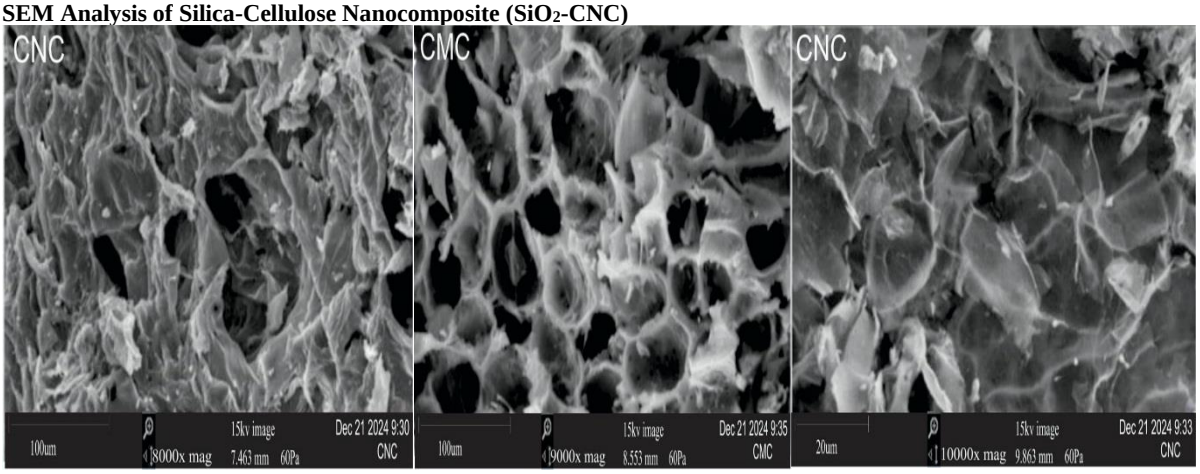

(a) (b) (c)

Figure 2: SEM analysis of silica-cellulose nanocomposite at different magnifications: (a) 8000x, (b) 9000x, and (c) 10000x

The scanning electron microscopy (SEM) analysis of the synthesized silica-cellulose nanocomposite (SiO_2-CNC) provides comprehensive insights into its structural and morphological characteristics across multiple magnification levels (8000x, 9000x, and 10000x). The progressive examination reveals a sophisticated material structure with features that demonstrate successful synthesis and integration of components, warranting detailed discussion of its morphological characteristics and potential applications. Initial examination at 8000x magnification (Fig. 2A) demonstrates the fundamental features of the nanocomposite, characterized by a fibrous structure with irregularly arranged layers forming a distinct porous network. This confirms the structural uniformity of the material with compositional uniformity, thus supporting the existence of successful synthesis methodology of the material (Anžlovar & Žagar, 2022). At 9000x magnification, further analysis (Fig. 2B) exposes fine particulars of the material microstructure with regard to the elaborated three-dimensional interconnected framework with the well-defined pore walls. The research shows that the material has a complex interconnected structure, with a highly defined, wrinkled, dry sheet surface texture that suggests the successful combination of silica and cellulose at the nanoscale (Ruiz-Palomero *et al*., 2017). The presence of rough and smooth surface regions suggests that there are differences in the bonding between cellulose and silica within the matrix, which increases the overall stability and functionality of the material. (Norizan *et al.,* 2022). The composite's structure at the highest magnification of 10000x (Fig. 2C) was exposed in the most detail, allowing for the discovery of very thin, flat, shard-like formations scattered over the entire composite material. This, in turn, indicates that there are crystalline or dense regions buried within the material matrix. This level of magnification focuses on the structure of the pores as well, particularly their arrangement in the nanocomposites, which indeed is correct in all levels of magnification (Cheung, 2018). The presence of small-scale porosity weakly visible at this level suggests pore creation on the nanoscale, which poses great opportunities for advanced applications (Harito *et al.,* 2019). An important observation is that the porosity of the material is uniformly distributed, and the pores are highly irregular in shape and size while maintaining a high degree of connectivity. The rough surface of the septa separating the pores is evidence of a high surface area (Janmohammadi *et al.,* 2023). Smoother regions amid the rough surfaces indicate areas of strong silica–cellulose interaction (Ogundare & van Zyl, 2019). Effective dispersion of silica in the cellulose matrix is evidenced by the homogeneous texture and complete absence of large agglomerates (Zhang *et al.,* 2022). These observed structural features collectively indicate the successful development of a well-integrated nanocomposite particularly suited for applications requiring high surface areas. The similar features of the structure from all other magnification levels indicate a favorable component dispersion for wide range of applications such as catalysis, adsorption, and even as reinforcing materials. The in-depth studies confirm the synthesis of an advanced nanocomposite with promising industrial and technological applications and recommend further studies of its mechanical and functional properties. The hierarchical structure observed from macro to nanoscale suggests that the synthesis methodology effectively created a material with multi-level functionality. This comprehensive integration of features across different scales indicates potential for optimized performance in various applications, particularly those requiring controlled porosity and high surface area. These findings provide a strong basis for further development and optimization of silica-cellulose nanocomposites for specific industrial applications.

TEM analysis of silica-cellulose nanocomposite synthesized from rice husk (SiO_2-CNC)

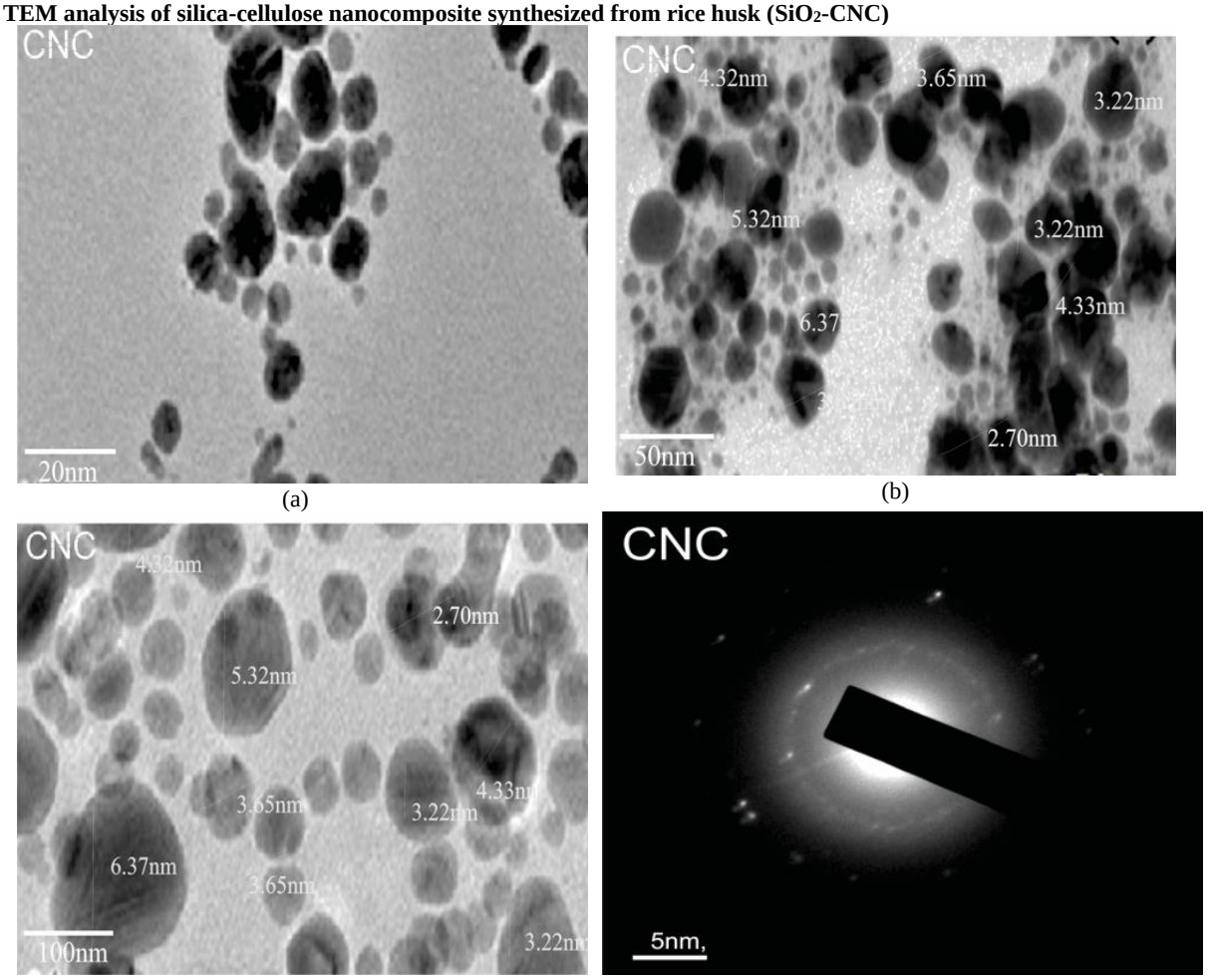

Figure 3: TEM analysis of silica-cellulose nanocomposite at different magnifications

The transmission electron microscopy (TEM) shows a comprehensive structural feature across the different magnification scales as shown in Fig. 3. Fig. 3A (20 nm) shows well-dispersed, spherical or near-spherical silica nanoparticles with dense silica cores, displaying clear contrast against the cellulose matrix (Njuguna *et al.,* 2021). The particle size distribution ranges from 2.70 nm to 6.37 nm, with most particles falling within the 3.22-5.32 nm range. The particle size ranges from 2.70 nm to 6.37 nm, and most particles are between 3.22 and 5.32 nm. At intermediate magnifications, Fig. 3B (50 nm) and Fig. 3C (100 nm) depict a wider view of the morphology and distribution of the particles. These magnifications reveal the spherical shape of the particles with defined boundaries and uniform spacing between them. The shape of the particles is highly consistent with a high degree of non-aggregation, which is important for understanding the spatial ordering and structural configuration of the composite (Njuguna *et al.,* 2021). The non-uniform distribution of particle sizes creates a synergistic dimension where the smaller particles occupy the spaces between the larger particles, which makes the material denser and stronger (Ahmed *et al.,* 2023). These observations across different magnification scales confirm the successful synthesis of a well-structured nanocomposite with controlled features at the nanoscale level, suggesting potential applications in areas requiring high surface area, controlled porosity, and stable nanostructured materials.

The Differential Thermal Analysis (DTA)/ Thermal Gravimetric Analyses of Silica-Cellulose Nanocomposite (SiO_2-CNC)

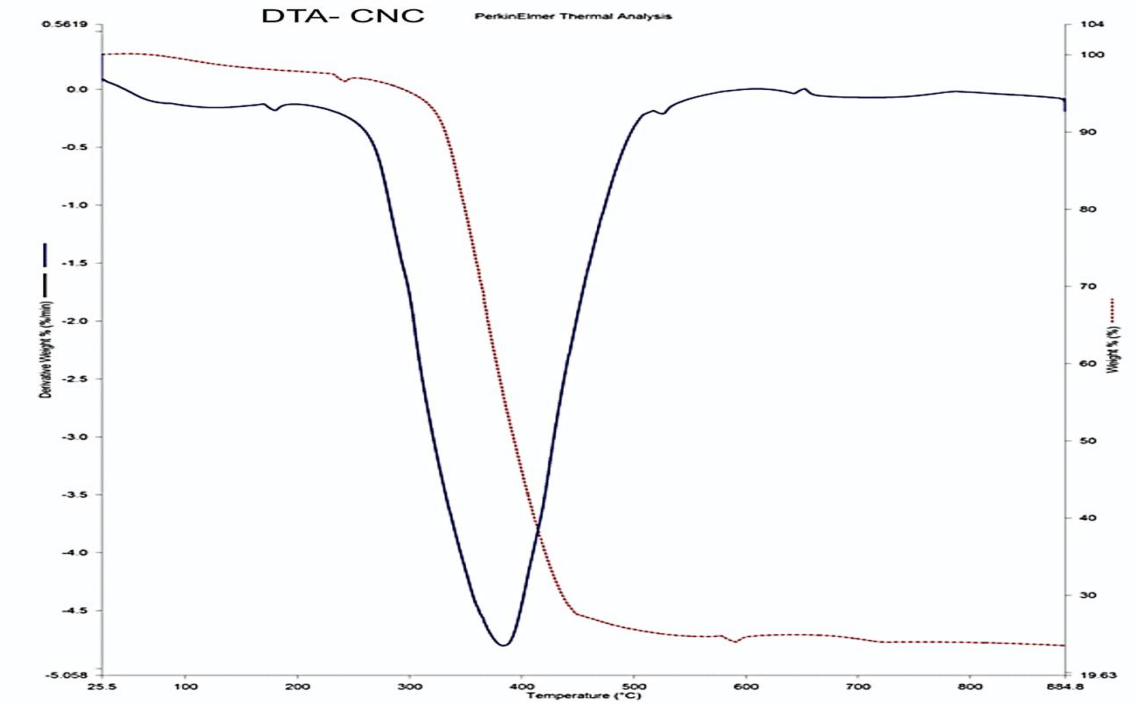

Figure 4: The Differential Thermal Analysis (DTA)/ Thermal Gravimetric Analyses (TGA) of silica-cellulose nanocomposite

The Differential Thermal Analysis (DTA) and Thermogravimetric Analysis (TGA) of the silica-cellulose nanocomposite derived from rice husk collectively provide a comprehensive understanding of its thermal behaviour, decomposition stages, and stability characteristics (Kumar *et al.*, 2024). The DTA and TGA of silica-cellulose nanocomposite using rice husk enables one to ascertain information with respect to the thermal properties, decomposition stages, and the stability attributes of the composite material (Corobea *et al.*, 2016). As shown in Fig. 4, in the initial phase (25–200°C), both DTA and TGA analyses reveal a modest weight loss of approximately 2-3%, attributed to the evaporation of absorbed moisture and volatile compounds. The gentle slopes in these regions point towards the thermal stability of the composite and the presence of well-bound water molecules in various binding environments (Agnello *et al.*, 2017), while the major decomposition phase of (200–400°C) reveals the most significant thermal event observed between 300-400°C, where a sharp endothermic peak (DTA) and dramatic weight loss (TGA) are recorded. There were weight decreases substantially, with 50-60% loss in DTA and a rapid decline from 95% to 30% in TGA. The climax of this stage corresponds to the breakdown of cellulose, with organic components being transformed into levoglucosan and other by-products through processes like depolymerisation and thermal disintegration (Nurazzi *et al.*, 2021). The high-temperature stabilization phase (400–894.8°C) occurs beyond 400°C; both analyses show a gradual weight loss with stabilization occurring above 500°C. The composite's high content of silica confirms its thermal stability as well as its resistance to decomposition beyond the organic phase, and the residual mass of approximately 20-25% can be attributed to the silica content, which acts as a thermal barrier and provides structural stability at elevated temperatures (Fu *et al.*, 2018). The presence of silica in the cellulose matrix, which improves thermal stability, is established by the merged DTA and TGA profiles. The thermal behaviour is characteristic of cellulose-based materials reinforced with silica, with distinct decomposition stages and a significant residual mass. The material exhibits thermal stability up to 250°C, making it suitable for applications requiring moderate temperature resistance, while the presence of silica ensures resistance at higher temperatures. These analyses provide valuable insights into the composite's thermal properties, processing requirements, and potential applications, validating its suitability for high-temperature and thermally stable environments.

Antioxidant of integrated cellulose nanocomposite

The in-vitro antioxidant activities of the silica nanocomposite from rice husk incorporated with *Callistemon citrinus* (SiO2-CNS) were evaluated using DPPH radical scavenging test. The DPPH assay is based on the reduction of DPPH radical to DPPH-H, which is indicated by a color change from violet to yellow in the presence of antioxidant compounds, due to the interaction with unpaired nitrogen electrons when dissolved in DMSO (Larayetan *et al*., 2017).

Table 1: The Si-CNS concentrations and their corresponding inhibition percentages for the DPPH and ABTS assays, including the standard deviations

SiO_2-CNS Concentration	DPPH Inhibition (%)	ABTS Inhibition (%)
20 mg/mL	86.15 ± 0.10	60.95 ± 0.15
10 mg/mL	62.69 ± 0.24	59.42 ± 0.15
5 mg/mL	45.33 ± 0.06	40.63 ± 0.10

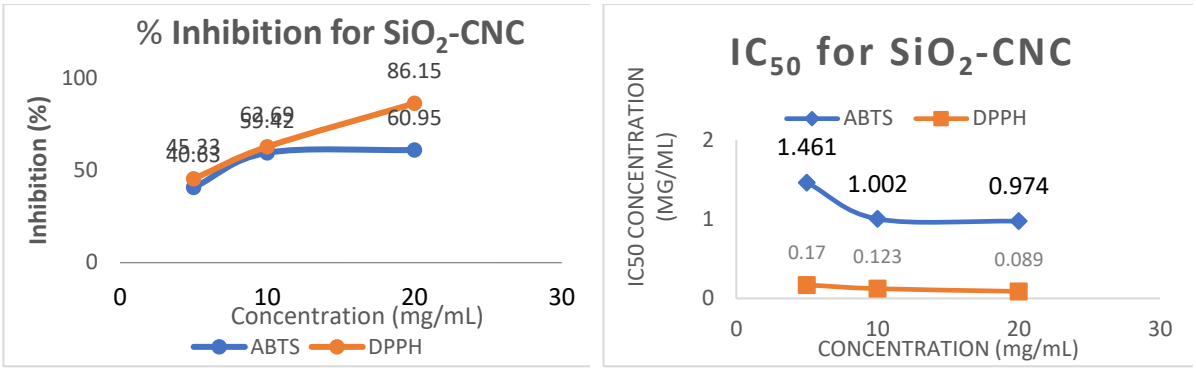

(a) (b)

Figure 5: Dose-dependent Inhibition and IC_{50} of DPPH and ABTS for SiO_2-CNS

The antioxidant activity of SiO_2-CNS was evaluated using the DPPH and ABTS radical scavenging assays, which are widely accepted methods for assessing free radical neutralization. The DPPH assay is based on the ability of antioxidants to donate hydrogen atoms or electrons, reducing the stable purple DPPH radical to a neutral yellow DPPH-H molecule. Similarly, the ABTS assay measures the capacity of antioxidants to quench ABTS radicals, which also leads to a color change indicating radical neutralization, with antioxidant effectiveness expressed through IC_{50} values, indicating the concentration required to reduce radical absorbance by 50% (Larayetan *et al*., 2019). The antioxidant potential of SiO_2-CNS was assessed using DPPH and ABTS assays, with results presented in the table 1.

The results in Figure 6a show that the percentage inhibition of SiO_2-CNS for both DPPH and ABTS increased in a concentration-dependent manner. At 5 mg/mL, DPPH inhibition was recorded at 45.33% ± 0.06, increasing to 62.69% ± 0.24 at 10 mg/mL, and reaching a maximum of 86.15% ± 0.10 at 20 mg/mL. ABTS inhibition followed a similar trend but was consistently lower than DPPH, with 40.63% ± 0.10 at 5 mg/mL, 59.42% ± 0.15 at 10 mg/mL, and 60.95% ± 0.15 at 20 mg/mL, as presented in Table 1.

The IC_{50} values, illustrated in Figure 6b, further highlight the antioxidant potential of SiO_2-CNS integrated with *Callistemon citrinus*. The DPPH IC_{50} decreased from 0.170 mg/mL at 5 mg/mL to 0.089 mg/mL at 20 mg/mL, indicating improved radical scavenging efficiency at higher concentrations. In contrast, ABTS IC_{50} values started at 1.461 mg/mL at 5 mg/mL and dropped to 0.974 mg/mL at 20 mg/mL, suggesting that while ABTS inhibition was moderate, it was still effective. The DPPH IC_{50} range (0.089–0.170 mg/mL) indicates strong antioxidant potential, with SiO_2-CNS exhibiting greater radical scavenging activity in the DPPH assay compared to ABTS. While SiO_2-CNS did not surpass the standard drugs vitamin C (IC_{50}: 0.00015 mg/mL) or Trolox (IC_{50}: 1.187 mM) in scavenging efficiency, it still demonstrated significant antioxidant capacity. Some authors attribute the high antioxidant activity of SiO_2-CNS to the different bioactive compounds it contains (Larayetan *et al.*, 2024). It is believed that the antioxidant activity of SiO_2-CNS is enhanced due to the combined effect of these compounds and the nano-silica composite structure. The results demonstrate that SiO_2-CNS possesses powerful antioxidant properties, particularly in DPPH radical scavenging, where it outperforms conventional antioxidants like vitamin C. This suggests that the incorporation of *Callistemon citrinus* into silica nanocomposites from rice husk biomass creates a promising material for applications requiring natural antioxidant properties.

FTIR analysis of silica-cellulose nanocomposite synthesized from rice husk (SiO_2-CNC)

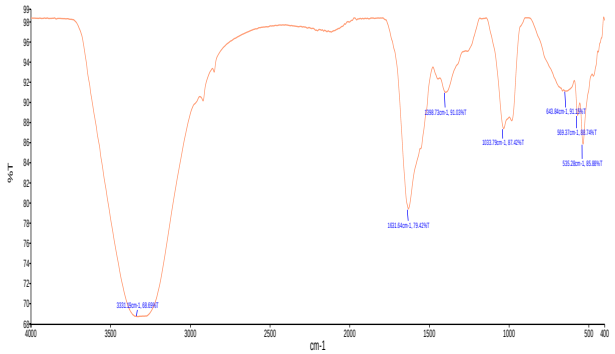

Figure 6a: FTIR of rice husk extract

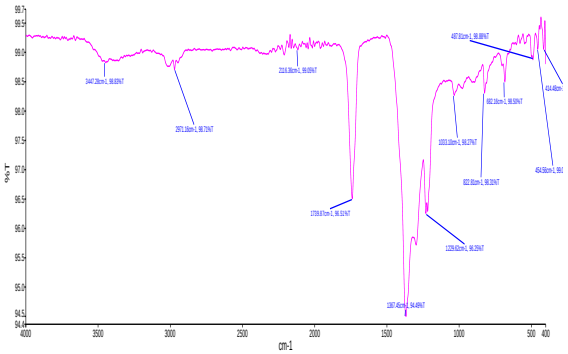

Figure 6b: FTIR of (SiO_2-CNC)

As seen in Fig. 6a, the organic substances found in rice husk extracts are abundant, including lignin, cellulose, hemicellulose, and a little amount of silica. Peaks that correspond to these components may be visible in the FTIR spectrum. As seen in Fig. 6a, the broad peak around 3331cm^{-1} indicates O-H stretching vibrations, suggesting the presence of alcohols or phenolic compounds (from lignin, cellulose, or water molecules) from the RH extract while peak around 2850–2950 cm^{-1} represents C-H stretching vibrations from aliphatic chains, common in cellulose and hemicellulose. Sharp needle-like peak around 1631 cm^{-1} suggests C=O stretching, which could arise from carboxylic acids, ketones, or esters in the organic matrix. In addition peaks in the range 1000–1250 cm^{-1} correspond to C-O stretching vibrations and Si-O-Si linkages, indicating both organic functionalities and silicates from the silica in rice husks. As seen in Fig. 6b, the fingerprint region (below 1500 cm^{-1}) contains complex vibrations from aromatic rings (lignin), C-H bending, and

polysaccharide components. As seen in Fig. 6b, the broad spectra O-H peak around 3447 cm^{-1} suggests the existence of organic residues, such as alcohols or phenolics, which stabilize the nanoparticles (Prema *et al.*, 2022). Also, the diminished C-H peak at about 2971 cm^{-1} is likely indicative of a lower quantity of aliphatic components after the vaporization of the extract when compared to its prior state (Li *et al.*, 2019). The broad spectra O-H peak around 3447 cm^{-1} suggests the existence of organic residues, such as alcohols or phenolics, which stabilize the nanoparticles (Prema *et al.*, 2022). Also, the diminished C-H peak at about 2971 cm^{-1} is likely indicative of a lower quantity of aliphatic components after the vaporization of the extract when compared to its prior state (Li *et al.*, 2019). Prominent Si-O peaks about 1000–1100 cm^{-1} reveal increased Si-O-Si vibrations, implying silica-based nanoparticles produced from the intrinsic silica in rice husk. A shift in the C=O peak at 1739 cm^{-1} might represent changes in oxidation states or functionalization of the surface during nanoparticle production. However, other peaks in the 400–800 cm^{-1} range could be signs of metal-oxide bonding, such as Si–O, Zn–O, or Fe–O (Miraftab *et al.*, 20217). Comparatively, it is possible that the O-H and C-H vibrations associated with lignin and cellulose in the rice husk extracts will be weaker in the silica-cellulose nanoparticle spectrum due to organic component degradation or removal while synthesizing the nanoparticles (Phong *et al.*, 2024). The FTIR spectra confirm the presence of functional groups in the rice husk extract that are associated with lignocellulose and silica, as well as the silica-cellulose nanoparticles; however, the silica-cellulose nanoparticle spectrum highlights the chemical transformations, particularly the loss of organic matter and the enhancement of silica or metal-oxide-related vibrations. The evidence suggests the nanoparticle synthesis was successful, and organic residues in the extract could permit the stabilization of the nanoparticles (Ovais *et al.*, 2018).

UV analysis of silica-cellulose nanocomposite synthesized from rice husk (SiO_2-CNC)

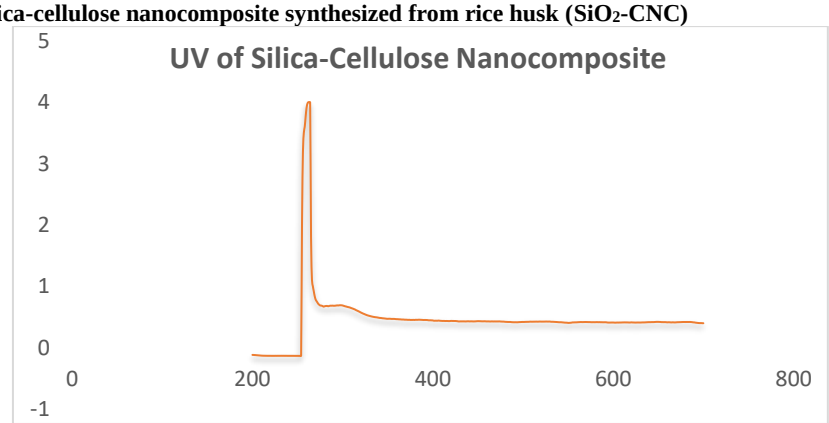

Figure 7: Uv-visible of Silica-Cellulose Nanocomposite

As shown in Fig. 7, the optical properties and surface modifications of the two components in the silica-cellulose composite contribute to the UV absorption band alteration. The peak at approximately 200-230 nm for the absorption in the silica-cellulose nanocomposite's UV spectrum is recommended for UV-blocking or filtering purposes. The silica component, which absorbs UV light in this region due to oxygen deficiency centres or surface defects in silica, is likely responsible for this strong absorption (Salh, 2018); cellulose may also contribute to this peak through $\pi \rightarrow \pi^*$ transitions from unsaturated or aromatic groups, if present (Zhang *et al.*, 2018). Also, beyond 300 nm, the absorption band decreased, thus the composite is almost transparent in the 300-700 nm visible region. Such behavior is anticipated because neither cellulose, nor silica, is known to have chromophores that would absorb in this region without being functionalized (Flematti, 2018). The flat baseline in the visible region of 400-800 nm indicates that there are no significant optical features in the visible range, which is typical for unmodified silica-cellulose composites. The transparency in the visible region suggests that the composite could be useful for optical applications where light transmission is desired (Dhatarwal *et al.*, 2021).

The optical characteristics of both components, as well as any surface alterations, affect the silica-cellulose composites' UV absorption band (Waleed *et al.*, 2025). UV radiation in the 200–300 nm range is absorbed by natural cellulose, with maxima usually occurring between 260 and 280 nm. Connected to unsaturated or aromatic groups' $\pi \rightarrow \pi^*$ transitions (if present in impurities or additives) (Ismail, 2023). Since it lacks chromophores, silica (SiO_2) is typically UV-transparent and does not absorb much beyond 200 nm (Mutailipu *et al.*, 2024). This is due to $n \rightarrow \pi^*$ transitions of carbonyl or other oxygen-containing compounds. However, modest absorption bands at 200–220 nm can be introduced by some silica structural defects, such as oxygen vacancies or surface silanol groups, because of oxygen shortage centers (Algar *et al.*, 2021). For silica-cellulose composites, the main UV absorption band usually falls between 200 and 300 nm, depending on the specific structure, composition, and any added functionalities (Lin *et al.*, 2021).

CONCLUSION

The study shows how agricultural waste can be successfully transformed into a material with added value and a variety of possible uses. The environmental issues surrounding the disposal of rice husks are addressed by this strategy, which also opens up possibilities for the development of cutting-edge materials with improved qualities. This work adds to the expanding field of sustainable nanomaterials and lays the groundwork for further investigation into bio-based nanocomposites with integrated functionality. These findings suggest that the silica-cellulose nanocomposite's functional characteristics particularly its antioxidant capacity are improved by the addition of *Callistemon citrinus*. Potential avenues for future research could include refining the synthesis procedure, investigating other functionalization techniques, and looking into particular uses in fields like UV protection, antioxidant delivery systems, and the creation of advanced materials.

REFERENCES

Agnello, S., Alessi, A., Buscarino, G., Piazza, A., Maio, A., Botta, L., & Scaffaro, R. (2017). Structural and thermal stability of graphene oxide-silica nanoparticles nanocomposites. *Journal of Alloys and Compounds*, *695*, 2054-2064.

Ahmed, H. U., Mohammed, A. A., & Mohammed, A. S. (2023). Effectiveness of silicon dioxide nanoparticles (Nano SiO2) on the internal structures, electrical conductivity, and elevated temperature behaviors of geopolymer concrete composites. *Journal of Inorganic and Organometallic Polymers and Materials*, *33*(12), 3894-3914.

Ahmed, M. (2019). Phenotypic and molecular identification of blast resistance genes in rice germplasm (Doctoral dissertation, MS Thesis, Sher-e-Bangla Agricultural University, Dhaka, Bangladesh).

Algar, W. R., Massey, M., Rees, K., Higgins, R., Krause, K. D., Darwish, G. H., ... & Kim, H. (2021). Photoluminescent nanoparticles for chemical and biological analysis and imaging. *Chemical Reviews*, *121*(15), 9243-9358.

Anžlovar, A., & Žagar, E. (2022). Cellulose structures as a support or template for inorganic nanostructures and their assemblies. Nanomaterials, 12(11), 1837.

Ates, B., Koytepe, S., Ulu, A., Gurses, C., & Thakur, V. K. (2020). Chemistry, structures, and advanced applications of nanocomposites from biorenewable resources. Chemical Reviews, 120(17), 9304-9362.

Bakare, W. A. (2021). Inter-Varietal Variation in Elemental Uptake by Rice and its Implications for Public Health: A Case Study of Dareta Village Zamfara State Nigeria. University of Salford (United Kingdom).

Balaji, D., Kumar, P. S., Bhuvaneshwari, V., Rajeshkumar, L., Singh, M. K., Sanjay, M. R., & Siengchin, S. (2024). A review on effect of nanoparticle addition on thermal behavior of natural fiber–reinforced composites. Heliyon.

Cheung, C. (2018). Fabrication of a porous anode with continuous linear pores by using unidirectional carbon fibers as sacrificial templates to improve the performance of solid oxide fuel cell. University of California, San Diego.

Corobea, M. C., Muhulet, O., Miculescu, F., Antoniac, I. V., Vuluga, Z., Florea, D., ... & Thakur, V. K. (2016). Novel nanocomposite membranes from cellulose acetate and clay-silica nanowires. *Polymers for Advanced Technologies*, *27*(12), 1586-1595.

Dairi, N., Ferfera-Harrar, H., Ramos, M., & Garrigós, M. C. (2019). Cellulose acetate/AgNPs-organoclay and/or thymol nano-biocomposite films with combined antimicrobial/antioxidant properties for active food packaging use. International Journal of Biological Macromolecules, 121, 508-523.

Dhatarwal, P., Choudhary, S., & Sengwa, R. J. (2021). Dielectric and optical properties of alumina and silica nanoparticles dispersed poly (methyl methacrylate) matrix-based nanocomposites for advanced polymer technologies. *Journal of Polymer Research*, *28*(2), 63.

FLEMATTI, C. (2018). Strategies for selective fluorescent functionalization of cellulose-based nanomaterials used for water remediation.

Fu, J. He, C., Wang, S., & Chen, Y. (2018). A thermally stable and hydrophobic composite aerogel made from cellulose nanofibril aerogel impregnated with silica particles. *Journal of Materials Science*, *53*, 7072-7082.

Ghosal, S., & Moulik, S. C. (2015). Use of rice husk ash as partial replacement with cement in concrete-A review. International Journal of Engineering Research, 4(9), 506-509.

Harito, C., Bavykin, D. V., Yuliarto, B., Dipojono, H. K., & Walsh, F. C. (2019). Polymer nanocomposites having a high filler content: synthesis, structures, properties, and applications. Nanoscale, 11(11), 4653-4682.

Hernandez Perez, R., Olarte Paredes, A., Salgado Delgado, R., & Salgado Delgado, A. M. (2023). Rice husk Var.'Morelos A-2010'as an eco-friendly alternative for the waste management converting them cellulose and nanocellulose. *International Journal of Environmental Analytical Chemistry*, *103*(19), 7571-7586.

Hernandez Perez, R., Olarte Paredes, A., Salgado Delgado, R., & Salgado Delgado, A. M. (2023). Rice husk Var.'Morelos A-2010'as an eco-friendly alternative for the waste management converting them cellulose and nanocellulose. *International Journal of Environmental Analytical Chemistry*, *103*(19), 7571-7586.

Ismail, M. (2023). Advanced imaging of lignocellulosic and cellulose materials.

Janmohammadi, M., Nazemi, Z., Salehi, A. O. M., Seyfoori, A., John, J. V., Nourbakhsh, M. S., & Akbari, M. (2023). Cellulose-based composite scaffolds for bone tissue engineering and localized drug delivery. Bioactive Materials, 20, 137-163.

Jannah, M., Ahmad, A., Hayatun, A., Taba, P., & Chadijah, S. (2019). Effect of filler and plastisizer on the mechanical properties of bioplastic cellulose from rice husk. Journal of Physics: Conference Series, 1341(3), 032019.

Khan, A., Rangappa, S. M., Siengchin, S., & Asiri, A. M. (Eds.). (2021). Biobased Composites: Processing, Characterization, Properties, and Applications. John Wiley & Sons.

Kuan, C. Y., Yuen, K. H., & Liong, M. T. (2012). Physical, chemical and physicochemical characterization of rice husk. British Food Journal, 114(6), 853-867.

Kumar, S., Prasad, L., Bijlwan, P. P., & Yadav, A. (2024). Thermogravimetric analysis of lignocellulosic leaf-based fiber-reinforced thermosets polymer composites: an overview. *Biomass Conversion and Biorefinery*, *14*(12), 12673-12698.

Larayetan, R. A., Okoh, O. O., Sadimenko, A., & Okoh, A. I. (2017). Terpene constituents of the aerial parts, phenolic content, antibacterial potential, free radical scavenging and antioxidant activity of Callistemon citrinus (Curtis) Skeels (Myrtaceae) from Eastern Cape Province of South Africa. BMC complementary and alternative medicine, 17, 1-9.

Larayetan, R., Ololade, Z. S., Ogunmola, O. O., & Ladokun, A. (2019). Phytochemical constituents, antioxidant, cytotoxicity, antimicrobial, antitrypanosomal, and antimalarial potentials of the crude extracts of Callistemon citrinus. *Evidence-Based Complementary and Alternative Medicine*, *2019*(1), 5410923.

Larayetan, R. A., Ayeni, G., Yahaya, A., Ajayi, A., Omale, S., Ishaq, U., ... & Enyioma-Alozie, S. (2021). Chemical composition of Gossypium herbaceum linn and its antioxidant, antibacterial, cytotoxic and antimalarial activities. *Clinical Complementary Medicine and Pharmacology*, *1*(1), 100008.

Larayetan, R., Friday, E. T., Oluranti, O., Owonikoko, Y., & Abdulrazaq, Y. (2024). Chemical Profile, Antitrypanosomal, Antiplasmodial and Antibacterial Activities of the Volatile Oil from the Seed of Callistemon Citrinus.

Li, Y., Liao, C., & Tjong, S. C. (2019). Synthetic biodegradable aliphatic polyester nanocomposites reinforced with nanohydroxyapatite and/or graphene oxide for bone tissue engineering applications. *Nanomaterials*, *9*(4), 590.

Lin, Z., Li, S., & Huang, J. (2021). Natural cellulose substance based energy materials. *Chemistry–An Asian Journal*, *16*(5), 378-396.

Miraftab, R., Ramezanzadeh, B., Bahlakeh, G., & Mahdavian, M. (2017). An advanced approach for fabricating a reduced graphene oxide-AZO dye/polyurethane composite with enhanced ultraviolet (UV) shielding properties: Experimental and first-principles QM modeling. *Chemical Engineering Journal*, *321*, 159-174.

Mohite, S. S., & Chavan, S. S. (2024). Synthesis and conjugation properties of alkynyl functionalized salicylidene Ni (II) and Zn (II) phosphine complexes and their use as a precursor for preparation of NiO and ZnO nanoparticles. *Inorganic and Nano-Metal Chemistry*, *54*(11), 1085-1096.

Moon, R. J., Martini, A., Nairn, J., Simonsen, J., & Youngblood, J. (2011). Cellulose nanomaterials review: structure, properties and nanocomposites. *Chemical Society Reviews*, *40*(7), 3941-3994.

Muthayya, S., Sugimoto, J. D., Montgomery, S, & Maberly, G, F. (2014). Academy of Science, 1324(1), 7-14.

Nguyen, N. T., et al. (2022). The extraction of lignocelluloses and silica from rice husk using a single biorefinery process and their characteristics. Journal of Industrial and Engineering Chemistry, 108, 150-158.

Njuguna, J., Ansari, F., Sachse, S., Rodriguez, V. M., Siqqique, S., & Zhu, H. (2021). Nanomaterials, nanofillers, and nanocomposites: types and properties. In *Health and environmental safety of nanomaterials* (pp. 3-37). Woodhead Publishing.

Norizan, M. N., Shazleen, S. S., Alias, A. H., Sabaruddin, F. A., Asyraf, M. R. M., Zainudin, E. S., ... & Norrrahim, M. N. F. (2022). Nanocellulose-based nanocomposites for sustainable applications: A review. Nanomaterials, 12(19), 3483.

Nurazzi, N., Asyraf, M. R. M., Rayung, M., Norrrahim, M. N. F., Shazleen, S. S., Rani, M. S. A., ... & Abdan, K. (2021). Thermogravimetric analysis properties of cellulosic natural fiber polymer composites: A review on influence of chemical treatments. *Polymers*, *13*(16), 2710.

Ogundare, S. A., & van Zyl, W. E. (2019). Amplification of SERS "hot spots" by silica clustering in a silver-nanoparticle/nanocrystalline-cellulose sensor applied in malachite green detection. Colloids and Surfaces A: Physicochemical and Engineering Aspects, 570, 156-164.

Oyejobi, D. O., Firoozi, A. A., Fernandez, D. B., & Avudaiappan, S. (2024). Integrating circular economy principles into concrete technology: Enhancing sustainability through industrial waste utilization. Results in Engineering, 102846.

Ovais, M., Khalil, A. T., Islam, N. U., Ahmad, I., Ayaz, M., Saravanan, M., ... & Mukherjee, S. (2018). Role of plant phytochemicals and microbial enzymes in biosynthesis of metallic nanoparticles. *Applied microbiology and biotechnology*, *102*, 6799-6814.

Patel, V. K., Singh, V. K., & Jendre, A. (2023). Role of secondary nutrient "sulphur" in oilseed crops. Int Year Millets, 2023, 27.

Phiri, R., Rangappa, S. M., Siengchin, S., Oladijo, O. P., & Dhakal, H. N. (2023). Development of sustainable biopolymer-based composites for lightweight applications from agricultural waste biomass: A review. Advanced Industrial and Engineering Polymer Research.

Phong, D. T., Tu, P. M., Dat, N. M., Nam, N. T. H., Cong, C. Q., Hai, N. D., ... & Hieu, N. H. (2024). Corn Stalk-Derived Cellulose Aerogel/Poly (vinyl alcohol): Impact of Hydrophobic Modifications on the Adsorption Activity and Assessment of Thermal Insulation Perspective. *Waste and Biomass Valorization*, *15*(12), 6959-6975.

Piyathissa, S. D. S., et al. (2023). Introducing a Novel Rice Husk Combustion Technology for Maximizing Energy and Amorphous Silica Production Using a Prototype Hybrid Rice Husk Burner to Minimize Environmental Impacts and Health Risk. Energies, 16(3), 1120.

Prema, P., Veeramanikandan, V., Rameshkumar, K., Gatasheh, M. K., Hatamleh, A. A., Balasubramani, R., & Balaji, P. (2022). Statistical optimization of silver nanoparticle synthesis by green tea extract and its efficacy on colorimetric detection of mercury from industrial waste water. *Environmental Research*, *204*, 111915.

Rehman, H. U., Aziz, T., Farooq, M., Wakel, A., & Rengel, Z. (2012). Zinc nutrition in rice production systems: a review. Plant and soil, 361, 203-226.

Reidy, B., Haase, A., Luch, A., Dawson, K. A., & Lynch, I. (2013). Mechanisms of silver nanoparticle release, transformation and toxicity: a critical review of current knowledge and recommendations for future studies and applications. Materials, 6(6), 2295-2350.

Requena, R., et al. (2019). Integral fractionation of rice husks into bioactive arabinoxylans, cellulose nanocrystals, and

silica particles. ACS Sustainable Chemistry & Engineering, 7(6), 6275-6286.

Ruiz-Palomero, C., Soriano, M. L., & Valcárcel, M. (2017). Nanocellulose as analyte and analytical tool: Opportunities and challenges. TrAC Trends in Analytical Chemistry, 87, 1-18.

Salh, R. (2011). Defect related luminescence in silicon dioxide network: a review. *Crystalline Silicon-Properties and Uses*, *135*, 172.

Salihu Makanta, A. (2021). Profiling of Selected Nigerian Local Rice Varieties for their Essential Trace Elements Content. School Of Physical Sciences Biennial International Conference (SPSBIC).

Shen, Y., Zhao, P., & Shao, Q. (2014). Porous silica and carbon derived materials from rice husk pyrolysis char. Microporous and Mesoporous Materials, 188, 46-76.

Teo, H. L., & Wahab, R. A. (2020). Towards an eco-friendly deconstruction of agro-industrial biomass and preparation of renewable cellulose nanomaterials: A review. International Journal of Biological Macromolecules, 161, 1414-1430.

Waleed, H., Hudaib, B., Al-Harahsheh, M., & Allawzi, M. (2025). Synthesis and Characterization of a Modified Silica/Cellulose Acetate Nanocomposite Ultrafiltration Membrane for Phenol Removal from Wastewater. *Separation and Purification Technology*, *353*, 128391.

Zhang, Y., Li, J., Gao, Y., Wu, F., Hong, Y., Shen, L., & Lin, X. (2022). Improvements on multiple direct compaction properties of three powders prepared from Puerariae Lobatae Radix using surface and texture modification: Comparison of microcrystalline cellulose and two nano-silicas. International Journal of Pharmaceutics, 622, 121837.

Zhang, C., Chao, L., Zhang, Z., Zhang, L., Li, Q., Fan, H., ... & Hu, X. (2021). Pyrolysis of cellulose: Evolution of functionalities and structure of bio-char versus temperature. *Renewable and Sustainable Energy Reviews*, *135*, 110416.

Mutailipu, M., Li, J., & Pan, S. (2024). Looking Back the Nonlinear Optical Crystals in a Functionalized Unit's Perspective. *Advanced Functional Materials*, 2419204.